Crystallization of purple nitrous oxide reductase from *Pseudomonas stutzeri*

Anja Pomowski,[a] Walter G. Zumft,[b] Peter M. H. Kroneck[b] and Oliver Einsle[a]*

[a]Lehrstuhl für Biochemie, Institut für Organische Chemie und Biochemie, Albert-Ludwigs-Universität Freiburg, Albertstrasse 21, 79104 Freiburg, Germany, and [b]Institut für Angewandte Biowissenschaften, Abteilung Molekulare Mikrobiologie, Karlsruher Institut für Technologie, Hertzstrasse 16, 76187 Karlsruhe, Germany

Correspondence e-mail: einsle@biochemie.uni-freiburg.de

Nitrous oxide reductase (N_2OR) from *Pseudomonas stutzeri* catalyzes the final step in denitrification: the two-electron reduction of nitrous oxide to molecular dinitrogen. Crystals of the enzyme were grown under strict exclusion of dioxygen by sitting-drop vapour diffusion using 2*R*,3*R*-butanediol as a cryoprotectant. N_2OR crystallized in either space group *P*1 or *P*6$_5$. Interestingly, the key determinant for the resulting space group was the crystallization temperature. Crystals belonging to space group *P*1 contained four 130 kDa dimers in the asymmetric unit, while crystals belonging to space group *P*6$_5$ contained a single dimer in the asymmetric unit. Diffraction data were collected to resolutions better than 2 Å.

1. Introduction

Nitrous oxide (N_2O) is one of the predominant 'greenhouse gases' and contributes to global warming with stratospheric ozone depletion (Ravishankara *et al.*, 2009). Even though the reduction of N_2O is highly exergonic, it is kinetically inert because of a high activation-energy barrier (Zumft & Kroneck, 2007). In bacteria that use nitrogen oxides instead of oxygen as terminal electron acceptors in respiratory metabolism, nitrous oxide is reduced to N_2 in a two-electron reaction by nitrous oxide reductase (NosZ), a soluble periplasmic enzyme that is characterized by its high sensitivity towards molecular dioxygen (Zumft, 1997).

Crystal structures of N_2OR have been described for the proteins from *Marinobacter hydrocarbonoclasticus* (formerly *Pseudomonas nautica*; Brown, Tegoni *et al.*, 2000; Brown, Djinovic Carugo *et al.*, 2000), *Paracoccus denitrificans* (Haltia *et al.*, 2003) and *Achromobacter cycloclastes* (Paraskevopoulos *et al.*, 2006), but all were obtained from enzyme isolated under aerobic conditions. They show a homodimeric protein of approximately 130 kDa with two distinct domains: an N-terminal seven-bladed β-propeller containing the unique tetranuclear Cu$_Z$ site and a C-terminal domain with a cupredoxin fold that contains the binuclear Cu$_A$ centre, a well studied electron-transfer site similar to that found in cytochrome *c* oxidase (Kroneck *et al.*, 1989). The enzyme as isolated aerobically was insensitive to dioxygen, but enzymatic activity was observed exclusively after complete reduction to an all-cuprous state (Dell'Acqua *et al.*, 2010). This activity required a strong reductant and was described by a concise mechanism that, however, is likely to be distinct from the action of anaerobically purified N_2OR, which is active in a more oxidized state (Ghosh *et al.*, 2003; Gorelsky *et al.*, 2006). Here, we describe the crystallization of the catalytically active purple form of the *Pseudomonas stutzeri* enzyme that was isolated under anaerobic conditions. The incentive of the work is to identify and understand possible structural or electronic differences between the different forms of the enzyme.

2. Methods

2.1. Crystallization

N_2OR crystals were obtained in a glove box with an N_2/H_2 (95%/5%) atmosphere, in which H_2 was used to react with residual oxygen

1541
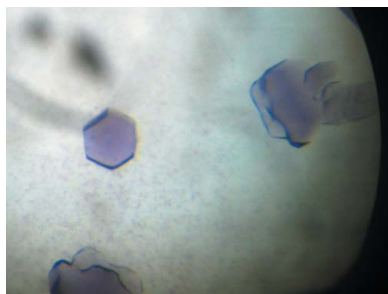
on a platinum catalyst surface and which contained <1 p.p.m. O_2. Crystals were grown by the sitting-drop vapour-diffusion method at 293 and 298 K (Fig. 1). The reservoir solution contained 16% polyethylene glycol 6000 and 0.2 M imidazole–malate buffer pH 7.0. 1 µl protein solution (15 mg ml^{-1}) was mixed with 1 µl reservoir solution and 2.8–4.5%(w/v) n-octyl-β-D-glucopyranoside was used as an additive.

For data collection, crystals were transferred to a harvesting buffer containing reservoir solution with 10%(v/v) 2R,3R-butanediol as a cryoprotectant. The crystals were subsequently flash-cooled in liquid nitrogen and were only then removed from the glove box.

2.2. Data collection and processing

Diffraction experiments were carried out on beamline X06SA (PXI) equipped with a Pilatus 6M detector at the Swiss Light Source (SLS), Villigen, Switzerland and on an in-house rotating copper-anode X-ray generator (Rigaku MicroMax-007 HF with MAR Research MAR345dtb image-plate system) at 100 K. The diffraction images were indexed and scaled using the programs *MOSFLM* and *SCALA* from the *CCP*4 package (Collaborative Computational Project, Number 4, 1994).

3. Results and discussion

Initial three-dimensional crystals growing as clusters were obtained from the Footprint sparse-matrix screen in a condition containing 16%(w/v) polyethylene glycol 4000 and 0.2 M imidazole–malate buffer pH 7.5. This condition was further refined by optimization of the PEG chain length, PEG concentration and buffer pH. Additives for crystallization were tried out in several rounds and in this process n-octyl-β-D-glucopyranoside was identified as a suitable agent to avoid the formation of crystal clusters.

Crystals with a purple colour appeared after approximately 2–4 d (Fig. 1). Depending on the temperature, the crystal morphology varied from cubes at 293 K to hexagonal shaped crystals at 298 K. The variation in crystal shape reflected the internal symmetry. The cubes belonged to space group $P1$, with unit-cell parameters $a = 96.9$, $b = 107.6$, $c = 131.1$ Å, $\alpha = 111.3$, $\beta = 107.3$, $\gamma = 90.7°$. For these crystals, diffraction data could be recorded to a resolution of 1.9 Å using an in-house rotating copper-anode generator at a wavelength of 1.5418 Å (Table 1). A calculation of the Matthews coefficient assuming a
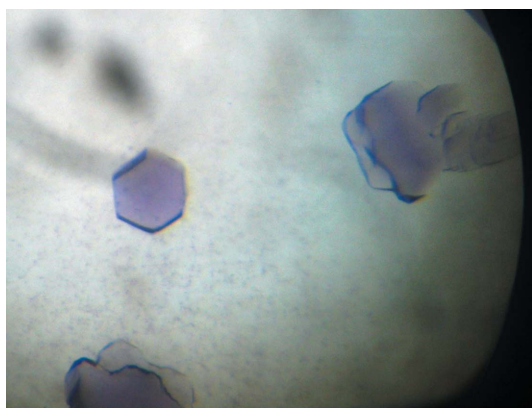
Table 1
Data-collection statistics.

Values in parentheses are for the highest resolution shell.

	Crystal form 1	Crystal form 2
Crystallization temperature (K)	293	298
Wavelength (Å)	1.5418	0.979
Space group	$P1$	$P6_5$
Unit-cell parameters (Å, °)	$a = 96.9$, $b = 107.6$, $c = 131.1$, $\alpha = 111.3$, $\beta = 107.3$, $\gamma = 90.7$	$a = b = 70.3$, $c = 399.7$
Resolution limits (Å)	50.0–1.9 (2.0–1.9)	50.0–1.7 (1.8–1.7)
Completeness (%)	94.7 (91.8)	98.3 (89.5)
Unique reflections	255620 (36175)	121422 (16139)
Multiplicity	2.1 (2.0)	5.4 (3.9)
R_{merge}	0.107 (0.492)	0.096 (0.485)
Mean $I/\sigma(I)$	16.7 (1.8)	10.6 (2.0)

molecular mass of 130 kDa for the dimer suggested the presence of four dimers in the asymmetric unit, with a solvent content of 46.5%.

The hexagonal crystals that appeared at the higher temperature belonged to space group $P6_5$, with unit-cell parameters $a = b = 70.3$, $c = 399.7$ Å, $\alpha = \beta = 90$, $\gamma = 120°$ and one dimer per asymmetric unit. Diffraction data were collected on beamline X06SA at SLS at a wavelength of 0.979 Å to a limiting resolution of 1.7 Å. The crystal showed clear signs of merohedral twinning, with two twin domains and likely twinning operation $-h - k, k, -l$. The transition between the two crystal forms was not an absolute one when crystallized at 293 K compared with 298 K, but rather consisted of a distinct shift of the preferred form, with various drops frequently containing both forms.

In both cases a molecular-replacement solution could be obtained with *Phaser* (McCoy *et al.*, 2007) using the model of nitrous oxide reductase from *Paracoccus denitrificans* as a search model (PDB code 1fwx; Brown *et al.*, 2000). For the $P1$ cell, four dimers of nitrous oxide reductase were placed using the same rotation-function solution in each case. This was highly indicative of the presence of translational pseudosymmetry, which should be reflected in a significant off-origin peak in native Patterson maps of the two crystals. The highest peak in
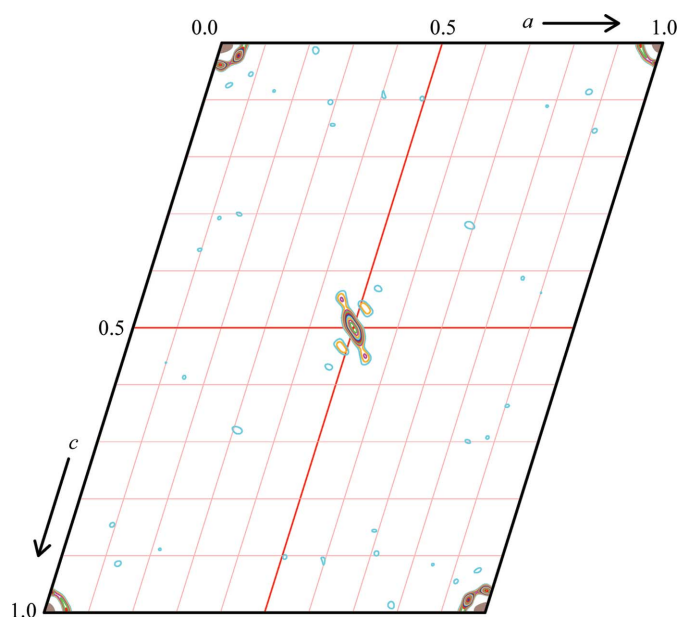

Figure 1
Crystals of purple *P. stutzeri* nitrous oxide reductase obtained at 298 K. As indicated by the crystal shape, this crystal form belongs to a hexagonal crystal system.

Figure 2
Plot of the $v = 0$ section of the native Patterson map of the $P1$ crystal form showing a moderate pseudo-origin peak at $u = w = 0.5$ with a total height of 8% of the origin peak. This figure was produced using *XPREP* (Bruker).

the map was found at (0.5, 0, 0.5), with 8% of the height of the origin peak (Fig. 2). In itself, this would not suffice to identify a pseudo-origin peak, but the position exactly corresponded to the interatomic vectors between the nitrous oxide reductase dimers. Further rigid-body refinement led to some tilting of the dimers in the model, which explains the relatively low height of the pseudosymmetry peak. Model building and refinement of *Pseudomonas stutzeri* nitrous oxide reductase are currently in progress.

References

Brown, K., Djinovic Carugo, K., Haltia, T., Cabrito, I., Saraste, M., Moura, J. J. G., Moura, I., Tegoni, M. & Cambillau, C. (2000). *J. Biol. Chem.* **275**, 41133–41136.

Brown, K., Tegoni, M., Prudencio, M., Pereira, A. S., Besson, S., Moura, J. J., Moura, I. & Cambillau, C. (2000). *Nature Struct. Biol.* **7**, 191–195.

Collaborative Computational Project, Number 4 (1994). *Acta Cryst.* D**50**, 760–763.

Dell'Acqua, S., Pauleta, S. R., Paes de Sousa, P. M., Monzani, E., Casella, L., Moura, J. J. & Moura, I. (2010). *J. Biol. Inorg. Chem.* **15**, 967–976.

Ghosh, S., Gorelsky, S. I., Chen, P., Cabrito, I., Moura, J. J. G., Moura, I. & Solomon, E. I. (2003). *J. Am. Chem. Soc.* **125**, 15708–15709.

Gorelsky, S. I., Ghosh, S. & Solomon, E. I. (2006). *J. Am. Chem. Soc.* **128**, 278–290.

Haltia, T., Brown, K., Tegoni, M., Cambillau, C., Saraste, M., Mattila, K. & Djinovic Carugo, K. (2003). *Biochem. J.* **369**, 77–88.

Kroneck, P. M. H., Antholine, W. A., Riester, J. & Zumft, W. G. (1989). *FEBS Lett.* **248**, 212–213.

McCoy, A. J., Grosse-Kunstleve, R. W., Adams, P. D., Winn, M. D., Storoni, L. C. & Read, R. J. (2007). *J. Appl. Cryst.* **40**, 658–674.

Paraskevopoulos, K., Antonyuk, S. V., Sawers, R. G., Eady, R. R. & Hasnain, S. S. (2006). *J. Mol. Biol.* **362**, 55–65.

Ravishankara, A. R., Daniel, J. S. & Portmann, R. W. (2009). *Science*, **326**, 123–125.

Zumft, W. G. (1997). *Microbiol. Mol. Biol. Rev.* **61**, 533–616.

Zumft, W. G. & Kroneck, P. M. H. (2007). *Adv. Microb. Physiol.* **52**, 107–225.